

THE PENNSYLVANIA STATE UNIVERSITY
SCHREYER HONORS COLLEGE

DEPARTMENT OF PHYSICS

SYNTHESIS AND CHARACTERIZATION OF SILICON DOPED SINGLE WALLED
CARBON NANOTUBES

JOHN SLIMAK
SPRING 2015

A thesis
submitted in partial fulfillment
of the requirements
for a baccalaureate degree
in Chemical Engineering
with honors in Physics

Reviewed and approved* by the following:

Mauricio Terrones
Professor of Physics, Chemistry, and Materials Science & Engineering
Thesis Supervisor

Richard Robinett
Professor of Physics
Honors Adviser

* Signatures are on file in the Schreyer Honors College.

ABSTRACT

Silicon doping of carbon nanotubes produces an isovalent structure, unlike that of similar boron or nitrogen doped tubes which display *p*- and *n*- characteristics, and causes unique structural changes to the nanotubes, altering the properties of both single tubes and bulk materials. Silicon doped single-walled nanotubes were prepared by chemical vapor deposition of ethanol vapor with catalytic ferrocene and methoxytrimethylsilane dopant. The material was characterized by Raman spectroscopy to determine the success of the synthesis and also to probe the diameter of the nanotubes; the presence of substitutional silicon atoms in the nanotube lattice create a preference for lower diameter tubes, a change that is easily observable through the radial breathing mode of the doped nanotubes.

TABLE OF CONTENTS

| | |
|--|-----|
| LIST OF FIGURES | iii |
| LIST OF TABLES | iv |
| ACKNOWLEDGEMENTS | v |
| Chapter 1 Introduction | 1 |
| Structure of Single-Walled Nanotubes..... | 2 |
| Electron and Phonon Properties of Single-Walled Carbon Nanotubes | 4 |
| Raman Spectroscopy | 6 |
| Silicon Doping of Single-Walled Carbon Nanotubes | 7 |
| Chapter 2 Experimental Methods | 9 |
| Chapter 3 Results and Discussion..... | 11 |
| Chapter 4 Conclusions and Further Work | 15 |
| BIBLIOGRAPHY..... | 16 |

LIST OF FIGURES

| | |
|---|----|
| Figure 1 - Carbon nanotube structure. (a) A zig-zag nanotube, (b) an armchair nanotube, (c) a chiral nanotube. (Source: Bandstructure of Graphen and Carbon Nanotubes: An Exercise in Condensed Matter Physics; developed by Christian Schönberger for MIT OpenCourseWare, April 2000) ⁸ | 3 |
| Figure 2 - Electronic band structure of graphene. (Source: Bandstructure of Graphen and Carbon Nanotubes: An Exercise in Condensed Matter Physics; developed by Christian Schönberger for MIT OpenCourseWare, April 2000) ⁸ | 4 |
| Figure 3 - Cutting lines on the Brillouin zone of a carbon nanotube. (Source: Bandstructure of Graphen and Carbon Nanotubes: An Exercise in Condensed Matter Physics; developed by Christian Schönberger for MIT OpenCourseWare, April 2000) ⁸ | 5 |
| Figure 4 - TEM images of SWNT Samples. (a) Undoped nanotubes exist singly, outside of bundles. (b-i) Doped nanotubes form bundles. | 11 |
| Figure 5 - D and G band Raman spectra of SWNTs. (a) A comparison of the peaks. (b) A plot showing the intensity ratio between D and G peaks as dependent on doping level..... | 12 |
| Figure 6 - Comparison of RBMs obtained at 514 nm laser excitation..... | 13 |
| Figure 7 - Plot of Raman Peaks and their intensities at different doping levels. | 14 |

ACKNOWLEDGEMENTS

First, I want to thank every member of my research group; in particular I owe a great debt to my research adviser, Dr. Terrones; Lakshmy Pulickal Rajukumar, the graduate student I had the privilege to work directly under; Dr. Ana Laura Elías, who for years has done such a wonderful job keeping me from losing my mind when my experiments failed; Dr. Eduardo Cruz Silva, whose emails always confused me when I expected them to come from Lalo, and who helped to ground me when I felt as though my world was falling apart during the graduate school application process. I owe much of my success to the great environment created by my lab group, which I will forever be thankful for.

I want to thank the people in my life who have stood by me through the entire ordeal that has been putting this together: my parents, John and Mary Kay Slimak, and my loving girlfriend Christina Nguyen. Were it not for all of your care and support through this entire process, from my first moments at Penn State to my final accomplishments, I do not know where I would be.

Chapter 1

Introduction

Following their initial discovery and structural characterization¹, carbon nanotubes have been actively researched in order to better understand their properties and to develop ways of altering those properties in order to expand their applicability in electronics and conducting composite materials. Properties of carbon nanotubes can be tuned by substitutional doping² which presents interesting opportunities for the introduction of novel characteristics by altering their electronic, mechanical, and chemical properties. Carbon nanotubes can be synthesized in a variety of ways, though the most common techniques are arc discharge^{3,4} and chemical vapor deposition² (CVD). In particular, CVD presents an easy method of producing substitutionally doped samples through the introduction of dopant compounds into solutions of carbon precursors and catalytic organometallics². Boron and nitrogen doping have been achieved in semiconducting nanotubes to produce p- and n- doped materials respectively².

With the intent to create covalently connected carbon nanotube networks that display inter-tube connections, we attempted to dope to single-walled carbon nanotubes with silicon, an isovalent atom with a strong preference for sp^3 hybridization rather than the sp^2 hybridization of the surrounding carbon atoms. The difference in hybridization means that the silicon atom both protrudes out from the surface of the nanotube by some distance and has an partially filled bonding orbital available as a chemically interactive site⁵. In the absence of other species, it is suspected that nearby silicon substitutions in other nanotubes will bond to form interconnections between the individual tubes, leading to networks of carbon nanotubes. Inter-tube bonding is expected to

improve conductivity of the nanotubes by enabling conduction across bundles of tubes, rather than exclusively along the translational vector of the tube. In addition, we expect the mechanical properties of the nanotubes to change due reduced ability of tubes to slip past each other.⁵

Structure of Single-Walled Nanotubes

Carbon nanotubes can be most easily related to graphene, which is the two dimensional parent crystal to a carbon nanotube; much of the theory of graphene can be applied to carbon nanotubes, simply by changing the boundary conditions associated with having a two dimensional crystal of graphene to having a sheet of graphene wrapped on itself.⁷ Based on the way the sheet is wrapped around to form the nanotube, different chiralities are observed – which in turn lead to differences in the electronic band structures and the properties of each . For example, some chiralities lead to SWNTs that are metallic in nature, while the others display semiconducting properties.⁷ The semiconducting or metallic character of the nanotube can be easily ascertained from the associated chiral vector, $\mathbf{C}_h = n\mathbf{a}_1 + m\mathbf{a}_2$, defined by the number of primitive lattice vectors in the graphene system needed to compose the unit cell for the one-dimensional carbon nanotube system.

The number of primitive lattice vectors in the graphene system contained in the chiral vector in the carbon nanotube system is often notated as (n, m); the chiral vector therefore has an associated angle, known as the chiral angle, defined as $\theta = \tan^{-1} \frac{\sqrt{3}m}{m+2n}$.⁷ For nanotubes with $\theta=30^\circ$ ($n=m$), the nanotube can be described as *armchair*; when $\theta=0^\circ$ ($m=0$) the tube is described as *zig-zag*; and for any values of θ between 0° and 30° the nanotube is known as chiral and can have some handedness (either left or right) associated with it. In the absence of magnetic fields, which break time-reversal symmetry in the system, the handedness can be neglected.

The diameter of a nanotube is given by $d_t = \frac{c_h}{\pi} = \frac{\sqrt{3}a_{CC}(m^2+mn+n^2)^{\frac{1}{2}}}{\pi}$, where a_{CC} is the distance between two adjacent carbons in graphene, 1.421 Å.⁷

To fully define the unit cell in the direct lattice of the carbon nanotube, we must consider the translational vector, defined by $\mathbf{T} = t_1\mathbf{a}_1 + t_2\mathbf{a}_2$, with the coefficients $t_1 = \frac{2m+n}{d_R}$ and $t_2 = -\frac{2n+m}{d_R}$ which are related to the coefficients of the chiral vector and where d_R is the greatest common divisor of $2n+m$ and $2m+n$.⁷

The unit cell of a carbon nanotube can thus be defined by either the diameter of the tube and the chiral angle or the chiral and translational vectors which serve as the lattice vectors in the carbon nanotube system.⁷

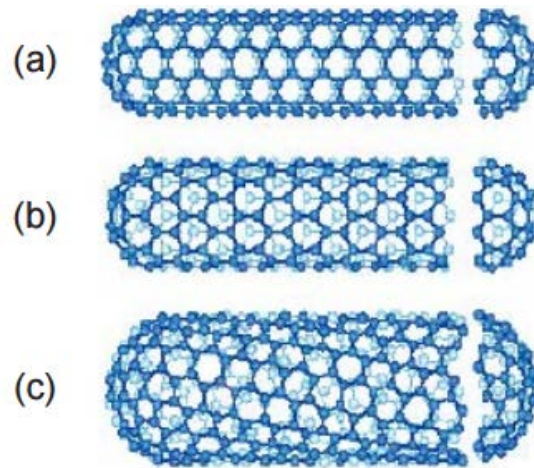


Figure 1 - Carbon nanotube structure. (a) A zig-zag nanotube, (b) an armchair nanotube, (c) a chiral nanotube. (Source: Bandstructure of Graphen and Carbon Nanotubes: An Exercise in Condensed Matter Physics; developed by Christian Schöenberger for MIT OpenCourseWare, April 2000)⁸

As the unit cell of a carbon nanotube is much larger than that of a graphene sheet, its Brillouin zone is significantly reduced in size in comparison to that of a graphene sheet. Defining the reciprocal lattice vectors can be done using the standard orthogonality conditions: $\mathbf{K}_1 \cdot \mathbf{C}_h = 2\pi$, $\mathbf{K}_1 \cdot \mathbf{T} = 0$, $\mathbf{K}_2 \cdot \mathbf{C}_h = 0$, and $\mathbf{K}_2 \cdot \mathbf{T} = 2\pi$.⁷

While the 2-dimensional electronic structure of graphene provides an excellent starting point for analysis of the band structure of carbon nanotubes, 1-dimensional confinement must be taken into account.⁷ Taking confinement into account results in specific “cutting lines” which can be applied to the usual 2-dimensional band structure for graphene, and then further modified by following the typical zone-folding scheme to reduce the domain of the graphene band structure into that of the carbon nanotube.^{7,9}

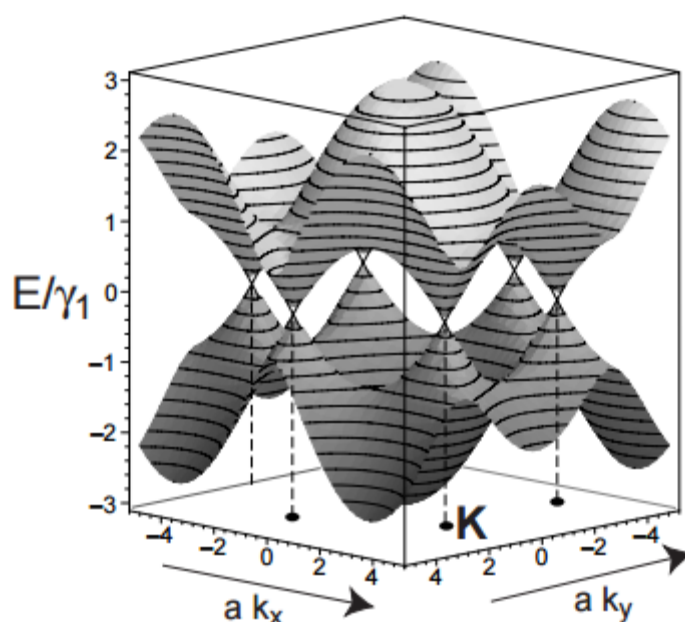


Figure 2 - Electronic band structure of graphene. (Source: Bandstructure of Graphen and Carbon Nanotubes: An Exercise in Condensed Matter Physics; developed by Christian Schönberger for MIT OpenCourseWare, April 2000)⁸

Electron and Phonon Properties of Single-Walled Carbon Nanotubes

Carbon nanotubes display differing electronic properties based on the placement of the cutting lines along the 2-D graphene band structure, resulting in either semiconducting or metallic characteristics: nanotubes with $(2n+m) \bmod 3 = 0$ are metallic in nature, though only when $n = m$

are they truly metallic, as others display a very small bandgap on the order of meV; in the cases when $(2n+m) \bmod 3$ is nonzero, the nanotubes display semiconducting properties and have a marked bandgap.⁷

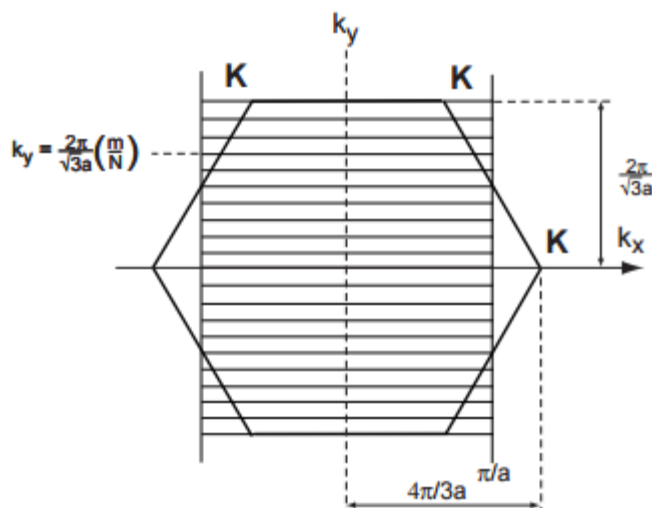


Figure 3 - Cutting lines on the Brillouin zone of a carbon nanotube. (Source: Bandstructure of Graphen and Carbon Nanotubes: An Exercise in Condensed Matter Physics; developed by Christian Schönberger for MIT OpenCourseWare, April 2000)⁸

In comparison to graphene with only 6 phonon modes, carbon nanotubes display significantly more due to the presence of many more than two atoms in the basis for their unit cells.⁷ The typical modes associated with in plane motion can be observed in the phonon dispersion relations for nanotubes, though there are many more than just 6; the number of dispersion relations is dependent on the number of atoms in the unit cell for the nanotube. In addition to the in-plane vibrational modes, carbon nanotubes also display phonon modes associated with rotation about the central axis, ones associated with “squashing” of the tube, and ones associated with radial expansion and contraction, or radial breathing, of the tube.^{7,10} The frequency associated with these radial breathing mode excitations, or the stretching of the nanotube perpendicular to the axis of the

nanotube, or RBMs, are characteristic of the nanotube's diameter in approximately an inverse relationship given by $\omega_{RBM} = c_1 + \frac{c_2}{d_t}$, where c_1 and c_2 are empirically determined constants.⁷

Raman Spectroscopy

Raman spectroscopy is a technique involving the use of a monochromatic light, typically a laser, to probe the vibrational excitations of a sample. In the case of carbon nanotubes, Raman spectroscopy is one of the most widely used and most important techniques for characterizing the structure of nanotubes and their phonon modes; in particular Raman spectroscopy allows for clear observation of the RBMs of a sample of nanotubes^{7,10}.

Raman scattering is the inelastic scattering of incident photons by phonons in the system being probed. Scattered photons are collected and those that scattered only elastically are filtered out, leaving a spectrum of photons with energies differing in energy from the incident photons by the energy absorbed into the varied phonon modes of the system. The intensity of peaks is dependent on the resonance of the incident or scattered light with the states of the system; resonant photons scatter much more intensely.^{7,10,12}

The Raman spectra of single-walled carbon nanotubes has several important features, though most are shared with graphene.⁷ The G and D bands, or graphitic and disorder bands, are Raman peaks associated with the carbon-carbon bond stretching in the sp^2 carbon sheet and disorder or defects in the sheet respectively. In addition to the G band, the G' band occurs at a higher energy than the G band and involves a double resonance process with phonons at the K point in the graphene Brillouin zone. For perfect samples of graphene, there should be little to no D peak observable. In the case of carbon nanotubes, the defect peaks are often associated with

doping or structural changes in the carbon nanotube.^{7,11,12} Unique to carbon nanotube Raman spectra are the RBM peaks, which appear at approximately $248/d_t$ cm^{-1} for a SWNT with diameter d_t nm.^{7,10}

Silicon Doping of Single-Walled Carbon Nanotubes

Doping of carbon nanotubes is often performed to tune the properties of the nanotubes using a diverse set of different atoms like boron, nitrogen, or phosphorus.^{2,13} These atoms substitute for carbon atoms in the nanotube lattice, and either introduce electrons or a holes into the electronic structure of the system. These materials can also display wildly different morphologies from standard single-walled carbon nanotubes. In the case of boron doping of multi-walled carbon nanotubes, the formation of kinks in the usually linear structure of the nanotube results in a macroscopic morphology resembling a sponge, with pores that are capable of absorbing a large volume of liquid.²

A new area of investigation is the doping of carbon nanotubes with silicon atoms, which are isovalent to carbon and therefore do not introduce *p*- or *n*- character to the material. Instead, it is expected that the silicon substitutional impurity will contribute a bonding site to the typically inert nanotube. Silicon is most stable in its sp^3 hybridized state, meaning that it protrudes from the surface of the carbon nanotube; sp^2 bonds are planar, while the sp^3 hybridized silicon will be have a tetrahedral geometry, projecting the silicon atom out of the regular cylindrical surface of the nanotube. As the silicon atom will also present a partially filled sp^3 orbital to the outside of the nanotube, it is expected to act as an amphoteric site for bonding.⁵ In this experiment we expect

nearby silicon atoms to preferentially bond to each other in the absence of other contaminants and in doing so create a 3-dimensional network of nanotubes.

First principles density functional theory calculations on (6,6) and (10,0) nanotubes revealed that the presence of silicon substitutions introduced changes into the local density of states of the nanotubes with respect to the undoped samples. A new localized level appears at 0.6 eV above the top of the valence band for the (10,0) semiconducting tube, and a resonating level is creating at 0.7 eV above the Fermi level for the (6,6) metallic tube.⁵

There are various consequences of successfully doping carbon nanotubes with silicon that can be investigated experimentally to confirm the presence of substitutional doping. The formation of silicon doping sites in the nanotube lattice is curvature dependent¹⁴: nanotubes with higher curvature have lower formation energies. As the curvature of the tube is inversely dependent on the size of the tube, we expect that successful silicon doping of carbon nanotubes will cause a shift in the distribution of the diameters of nanotubes present in the synthesized samples toward lower diameters. In addition, we expect an increase in the intensity of the D band of the Raman spectra related to the presence of defects in the tube. Variable range hopping theory also presents a further test of doping: if the tubes are present in a network, we expect a temperature dependence corresponding to 3-dimensional conduction for the conductivity of the doped materials with respect to the pristine materials.¹⁵

Chapter 2

Experimental Methods

Following the procedure of Lupo et al.¹⁷, solutions of ethanol and ferrocene were prepared by dissolving 2.99 g of ferrocene in 300mL of ethanol and sonicating until no visible particles solute were present. Varying amounts of methoxytrimethylsilane (MTMS) were added to the precursor solutions to produce solutions of 0.03, 0.05, 0.06, 0.075, and 0.10 wt% solutions. In the case of pristine samples, no MTMS was added in order to produce undoped nanotubes for comparison with the doped samples. Aerosol assisted chemical vapor deposition (AACVD) was used to grow the samples on the interior of a quartz tube at a reaction temperature of 1000°C. Inert argon gas was used to purge the quartz tube reactor and assisted to flow the aerosol through the reactor. Flow of argon was held at a constant 0.5 L/min during the heating period of the tube furnace and upon reaching the reaction temperature, the flow rate was increased to 0.7 L/min and the ultrasonic generator was turned on to aerosolize the reaction mixture. SWNTs were collected from the tube walls after the reactor cooled to room temperature using a metal rod to twist the grey-black films formed into strands that were easily removed from the metal rod.

Raman spectroscopy was performed with a Renishaw inVia confocal micro-Raman spectrometer with a 50x objective. As the intensity of the Raman spectra for carbon nanotubes is dependent on resonance between the bandgap of the nanotubes and the incident light, samples were analyzed with 488 nm, 514 nm, 647 nm, and 785 nm wavelength laser light at 34mW of laser power. Spectra obtained were fitted using Lorentzian profiles for the RBM, D band, G band, and 2D band.

High Resolution Transmission Electron Microscopy (HRTEM) was performed using JEOL 2010F with a field emission source operating at 200kV. SWNTs were dispersed in acetone using

a horn sonicator for 10 minutes and then dropped onto 300 mesh holey carbon copper grids to obtain electron transparent samples.

Electrical resistivity measurements were performed using a Keithley 2400 Sourcemeter. Electrical contacts with the SWNT strands were made using copper wires and conductive silver paste. In order to study the temperature dependence of resistivity, a Lakeshore 331 temperature controller was used.

Chapter 3

Results and Discussion

Bundles of SWNTs were observed in all samples regardless of concentration of MTMS. In the pristine SWNT samples, the tubes can be seen to exist primarily as individual tubes, not bundled together tightly. In the case of the doped Si-SWNTs, however, the tubes appear to have coalesced into bundles of tubes. Transmission Electron Microscopy (TEM) images also reveal that more than 90% of the nanotubes observed in the samples are single-walled carbon nanotubes rather than multi-walled nanotubes, though in more highly doped samples, large spherical particles can be observed as well. These spherical particles have been reported previously by Campos-Delgado et al.² and are believed to consist of metallic impurities from the iron-based catalyst, silicon oxides, and ternary compounds of silicon, iron, and oxygen. The density of tubes is much higher for lower dopant concentrations compared to the higher MTMS concentration samples.

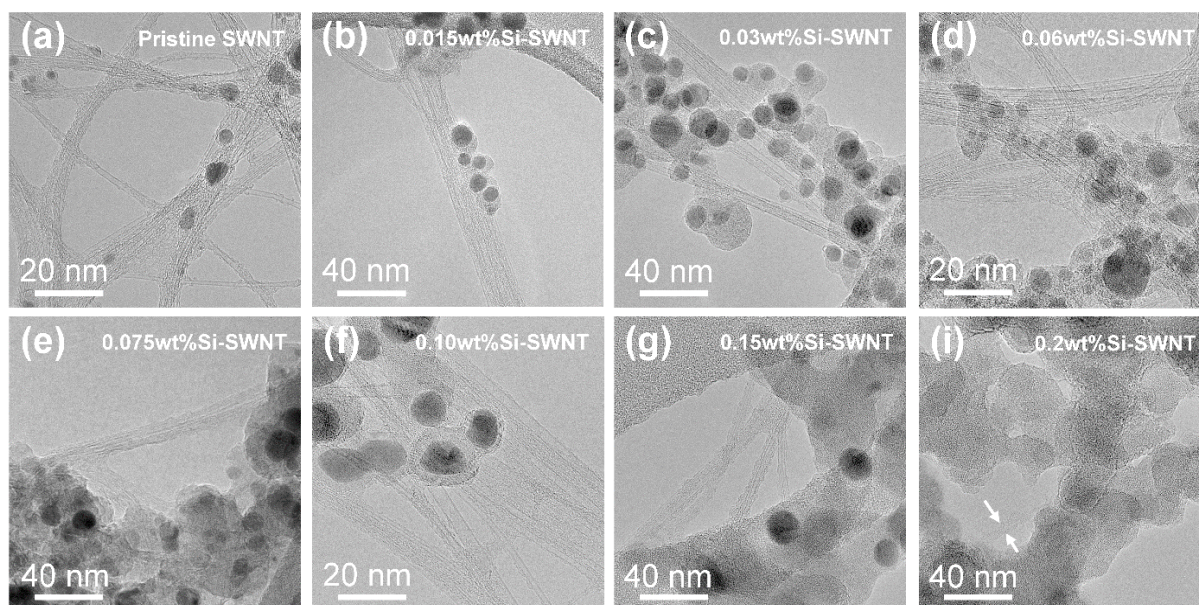


Figure 4 - TEM images of SWNT Samples. (a) Undoped nanotubes exist singly, outside of bundles. (b-i) Doped nanotubes form bundles.

While other peaks can help in showing that there has been an increase in the doping of the carbon nanotubes, there are some problems associated with using them even semi-quantitatively to determine the extent of the doping which can be better resolved through analysis of the RBMs of the samples. The G peak can be resolved into G^+ and G^- peaks in the spectra of each sample, which can be seen at approximately 1590 cm^{-1} and 1565 cm^{-1} respectively.¹⁰ While the G^+ peak is associated with carbon-carbon bond stretching, and therefore independent of the nanotube diameter, the G^- peak is associated with Breit-Wigner-Fano (BWF) resonance, a consequence of the interference between Raman scattering from continuum excitations and discrete phonons, and therefore exhibits diameter dependence for isolated SWNTs^{10,16}; we hope to find nanotubes in bundles, which unfortunately washes out the diameter dependence due to the close proximity of tubes of potentially varying diameters, meaning we cannot make determinations of the doping extent based on the G^- peak location or intensity.

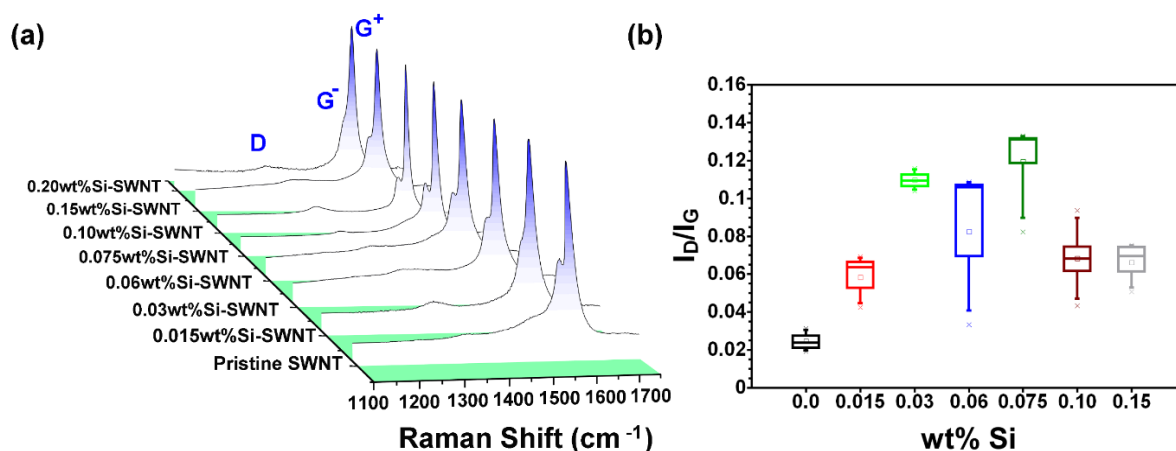


Figure 5 - D and G band Raman spectra of SWNTs. (a) A comparison of the peaks. (b) A plot showing the intensity ratio between D and G peaks as dependent on doping level.

As the D peak intensity is directly related to the amount of disorder in the SWNTs, it is directly related to the doping level of the tubes. In Figure 5 (b) it can be seen that with increasing

doping level, the ratio of the intensities of the D and G peaks increases, indicating that the introduction of additional MTMS is affecting the level of disorder in the SWNTs. While the D peak is also related to the diameter of the nanotubes¹⁰, it cannot be resolved well into individual peaks and suffers from the same problem as the G⁻ peak.

The RBMs offer us the only semi-quantitative method of analyzing the change in the diameters of the nanotubes. In Figure 6 there is a significant decrease in the peak intensities associated with higher diameter tubes (peaks with lower shift) when looking at the doped samples in comparison to the pristine SWNTs, and a complete loss of some of the peaks associated with the highest diameter SWNTs (peaks with the lowest shift).

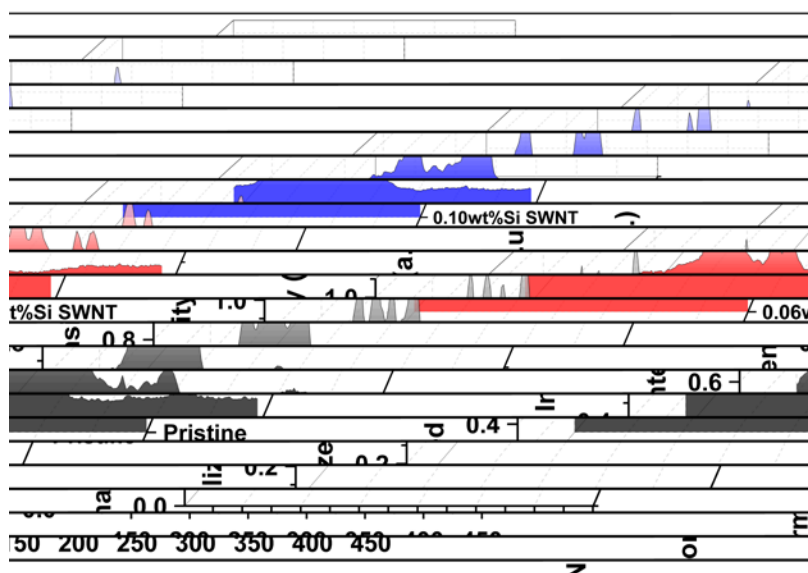


Figure 6 - Comparison of RBMs obtained at 514 nm laser excitation

In particular, the RBM measurements show a decrease in the intensity of peaks associated with tubes of diameters approximately 1.84 nm, 1.64 nm, 1.49 nm, 1.39 nm, and 1.33 nm, but a significant increase in the intensity of peaks associated with tubes of diameters approximately 1.00

nm and 0.95 nm. Figure 7 shows the shift in the peak intensities toward higher RBMs more clearly. The increase in the intensity of the peaks with lower diameter is interpreted as an increase in the quantity or concentration of the lower diameter tubes, which together with the TEM images strongly support the creation of nanotube bundles with silicon-silicon interconnections.

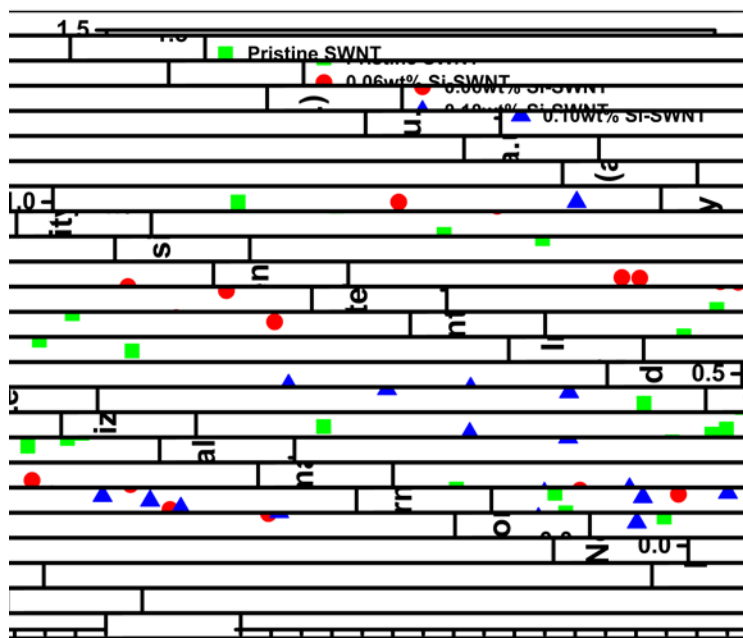


Figure 7 - Plot of Raman Peaks and their intensities at different doping levels.

Chapter 4

Conclusions and Further Work

The ultimate goal of this work was to create a network of carbon nanotubes connected by silicon-silicon bonds by performing the already established procedure to synthesize single-walled carbon nanotubes by AACVD of ethanol and ferrocene at 1000°C with a dopant of MTMS. The reaction produced a thin grey-black film on the interior of the quartz reaction tube in correspondence with the usual procedure, which was then wound out of the tube and saved for analysis following each reaction in the series of syntheses at increasing dopant levels. At first glance, the synthesis appeared to have successfully produced a sample of carbon nanotubes, and this was confirmed by analysis with TEM and Raman spectroscopy.

Confirmation of successful doping proved to be more intensive and required analysis of the RBMs of the samples. A trend was observed showing a decrease in the intensity of RBM peaks associated with tubes of higher diameters and an increase in the intensity of peaks associated with lower diameter tubes, in accordance with the proposed theory. Based on RBMs alone, it is not possible to conclusively say whether or not networks or bundles of tubes have formed, but the TEM images help to justify the conclusion that they have.

Further work can be done to assess the quality of the junctions or the extent to which inter-tube bonding has occurred by analyzing the electron transport mechanisms. While undoped nanotubes are expected to display 1-dimensional conduction, in accordance with the Variable Range Hopping theory, silicon doping should raise the dimensionality of the SWNTs to 3-dimensional. Preliminary investigations into the electrical transport mechanisms in silicon doped nanotubes are underway.

BIBLIOGRAPHY

1. Iijima, S. Helical microtubules of graphitic carbon. *Nature* **354**, 56-58 (1991).
2. Campos-Delgado, J., *et al.* Chemical vapor deposition synthesis of N-, P-, Si-doped single-walled carbon nanotubes. *ACS Nano* **4**, 1696-1702 (2010).
3. Terrones, M. *et al.* *Recent Advances in the Chemistry and Physics of Fullerenes and Related Materials Vol. 2*(eds Kadish, K. M. & Ruoff, R. S.) 599–620 (Electrochem. Soc., Pennington, NJ, (1995)).
4. Ebbesen, T. W. & Ajayan, P. M. Large scale synthesis of carbon nanotubes. *Nature* **358**, 220–222 (1992).
5. Baierle, R. J., Fagan, S. B., Mota, R., da Silva, A. J. R. & Fazzio, A. Electronic and structural properties of silicon-doped carbon nanotubes. *Phys. Rev. B* **64**, 085413 (2001).
6. Kis, A., Csányi, G., Salvetat, J.-P., *et al.* Reinforcement of single-walled carbon nanotube bundles by intertube bridging. *Nature Materials* **3**, 153-157 (2004).
7. Dresselhaus, M. S., Dresselhaus, G., Saito, R., Jorio, A. Raman spectroscopy of carbon nanotubes. *Physics Reports* **409**, 47-99 (2005).
8. Allan Adams, Matthew Evans, and Barton Zwiebach. 8.04 Quantum Physics I, Spring 20 (Massachusetts Institute of Technology: MIT OpenCourseWare), <http://ocw.mit.edu> (Accessed 7 Apr, 2015). License: Creative Commons BY-NC-SA
9. Samsonidze, Ge G., *et al.* The concept of cutting lines in carbon nanotube science. *Journal of Nanoscience and Nanotechnology* **3.6** (2003): 431-458.
10. Jorio, A., Saito, R., *et al.* Structural (n, m) determination of isolated single-wall carbon nanotubes by resonant Raman scattering. *Phys. Rev.* **86** 6 (2000)

11. Suzuki, S. & Hibino, H. Characterization of doped single-wall carbon nanotubes by Raman spectroscopy. *Carbon* **49**, 2264–2272 (2011).
12. Jorio, A., Pimenta, M. A., Souza Filho, A. G., Saito, R., Dresselhaus, G., Dresselhaus, M. S. Characterizing carbon nanotube samples with resonance Raman scattering. *New Journal of Physics* **5**, 139.1-139.7 (2003).
13. Cruz-Silva, E., Cullen, D. A., Lin, G., *et al.* Heterodoped Nanotubes: Theory, Synthesis, and Characterization of Phosphorus-Nitrogen Doped Multiwalled Carbon Nanotubes. *ACS Nano* **2008**, 441-448 (2008).
14. Fagan, S. B., Mota, R. da Silva, A. J. R., Fazzio, A. Substitutional Si doping in deformed carbon nanotubes. *Nano Letters* **4** (5), 975-977 (2004).
15. Shiraishi, M. Ata, M. Conduction mechanisms in single-walled carbon nanotubes. *Synthetic Materials* **128**, 235-239 (2002).
16. Eklund, P. C., Subbaswamy, K. R. Analysis of Breit-Wigner line shapes in the Raman spectra of graphite intercalation compounds. *Phys. Rev. B* **20**, 5157 (1979).
17. Lupo, F., *et al.* Pyrolytic synthesis of long strands of large diameter single-walled carbon nanotubes at atmospheric pressure in the absence of sulphur and hydrogen. *Chem. Phys. Letters* **410**, 384-390 (2005).

ACADEMIC VITA

John Edward Slimak II
112 Jefferson Street
Brookville, PA 15825
Jes5771@psu.edu / jeslimak@gmail.com

EDUCATION

B.S. Chemical Engineering with a minor in Physics
Pennsylvania State University, College of Engineering & Schreyer Honors College
University Park, PA
Honors in Physics
Thesis Title: Synthesis and Characterization of Silicon Doped Single-Walled Carbon Nanotubes
Thesis Supervisor: Mauricio Terrones

EXPERIENCE

Undergraduate Research Assistant – Physics Department, Eberly College of Science

- Synthesized samples of novel doped materials under the supervision of Dr. Mauricio Terrones.
- Characterized materials by Raman spectroscopy, SEM, and TEM in efforts to better understand and find applications for materials produced in laboratory conditions outside of the lab.

Polymer Adhesives Research Intern – Avery Dennison, Materials Group

- Developed new synthetic procedures at the laboratory scale for the production of a resealable adhesive for use in consumer products.
- Contributed as a team member on progress updates and a final presentation on the development of the above adhesive.
- Tested and characterized samples of adhesives produced in the lab using industry standard techniques.

Course Grader – Chemical Engineering Department, College of Engineering

- Graded for CHE 360, Mathematical Modeling in Chemical Engineering, under the supervision of Dr. Costas Maranas and Dr. Antonios Armaou.
- Graded for CHE 210, Introduction to Material Balances, under the supervision of Dr. Darrel Velegol.

HONORS

Eagle Scout Award, Boy Scouts of America
Schreyer Honors Scholarship, Schreyer Honors College
Schreyer Honors Summer Grant, Schreyer Honors College
John R. and Jeannette Dacheille McWhirter Scholarship
Howard L. Stethers Scholarship in Chemical Engineering
Larry B. Parsons Scholarship in Chemical Engineering
Helen Geist Scholarship in Chemical Engineering

ORGANIZATIONS

Penn State Quizbowl – President
Omega Xi Epsilon – Member
Nittany Chemical Society – Member
Penn State Club Kickball – Member